Reduced cardiac conduction velocity and predisposition to arrhythmias in connexin40-deficient mice

Susanne Kirchhoff*, Eric Nelles*, Andreas Hagendorff†, Olaf Krüger*, Otto Traub* and Klaus Willecke*

Intercellular channels of gap junctions are formed in vertebrates by the protein family of connexins and allow direct exchange of ions, metabolites and second messenger molecules between apposed cells (reviewed in [1–3]). In the mouse, connexin40 (Cx40) protein has been detected in endothelial cells of lung and heart and in certain heart muscle cells: atrial myocytes, cells of the atrial ventricular (AV) node and cells of the conductive myocardium, which conducts impulses from the AV node to ventricular myocyctes [3]. We have generated mice homozygous for targeted disruption of the *Cx40* gene (*Cx40*$^{-/-}$ mice). The electrocardiograph (ECG) parameters of *Cx40*$^{-/-}$ mice were very prolonged compared to those of wild type (*Cx40*$^{+/+}$) mice, indicating that *Cx40*$^{-/-}$ mice have lower atrial and ventricular conduction velocities. For 6 out of 31 *Cx40*$^{-/-}$ animals, different types of atrium-derived abnormalities in cardiac rhythm were recorded, whereas continuous sinus rhythm was observed for the 26 *Cx40*$^{+/+}$ and 30 *Cx40*$^{+/-}$ mice tested. The expression levels of other connexins expressed in heart (Cx37, Cx43 and Cx45) were the same in *Cx40*$^{-/-}$ and *Cx40*$^{+/+}$ mice. Our results demonstrate the function of Cx40 in the regulation and coordination of heart contraction and show that cardiac arrhythmogenesis can not only be caused by defects in the ion channels primarily involved in cellular excitation but also by defects in intercellular communication through gap junction channels. As the distribution of Cx40 protein is similar in mouse and human hearts, further functional analysis of Cx40 should yield relevant insights into arrhythmogenesis in human patients.

Addresses: *Institut für Genetik, Abt. Molekulargenetik, Universität Bonn, Römerstr. 164, 53117 Bonn, Germany. †Medizinische Klinik, Innere Medizin Kardiologie, Universität Bonn, Sigmund-Freud-Str. 25, 53105 Bonn, Germany.

Correspondence: Klaus Willecke
E-mail: genetik@uni-bonn.de

Received: 10 December 1997
Revised: 12 January 1998
Accepted: 20 January 1998

Published: 16 February 1998

Current Biology 1998, 8:299–302
http://biomednet.com/elecref/0960982200800299

Results and discussion

For targeted disruption of the mouse *Cx40* gene we used the targeting vector shown in Figure 1a. One chimeric mouse transmitted the disrupted *Cx40* allele through the germline, as confirmed by Southern blot and polymerase chain reaction (PCR) analysis (Figure 1b,c). Genotyping of the progeny after mating of *Cx40*$^{+/-}$ mice with mixed C57BL/6 × 129Sv background yielded 27% (38/139) *Cx40*$^{+/+}$, 54% (75/139) *Cx40*$^{+/-}$ and only 19% (26/139) *Cx40*$^{-/-}$ mice. *Cx40*$^{-/-}$ mice were fertile and had approximately the same body weight as wild-type and *Cx40*$^{+/-}$ littermates. *Cx40* mRNA was not detected in *Cx40*$^{-/-}$ mice and was less abundant in *Cx40*$^{+/-}$ mice than in wild-type controls, as assessed in lung and heart using the Del probe shown in Figure 1a for northern blot analyses (Figure 1d). No Cx40 protein was detected by immunoblot analysis of preparations from *Cx40*$^{-/-}$ lung enriched for gap junctions [4] (Figure 1e). Using this method, the amount of Cx40 protein found in heterozygous lung was less than half of that in wild-type tissue (Figure 1e). As the alkali insolubility method used enriches for large, rather than small, gap junction plaques, we may have lost part of the Cx40 protein during plaque enrichment.

Immunohistochemical analysis using an anti-Cx40 antibody on cryostat sections of coronary vessels and atrium revealed punctate gap junction labelling on contact membranes of the cells in wild-type mice (Figure 2a,g) but not in *Cx40*-deficient mice (Figure 2b,h). As Cx40 is co-expressed with Cx37 in endothelial cells, with Cx43 in atrium and with Cx45 in atrium and conductive myocardium [3], the viability of *Cx40*$^{-/-}$ mice might be due to an increase in the activity of these connexins such that they compensate for the absence of Cx40. Transcript and protein levels of these connexins remained unaltered, however, as revealed by northern blot analysis of Cx37, *Cx43* and *Cx45* transcripts and immunoblot analysis of Cx43 and Cx45 proteins in *Cx40*$^{+/+}$, *Cx40*$^{+/-}$ and *Cx40*$^{-/-}$ hearts as well as lungs (data not shown). The tissue distribution of Cx37, Cx43 and Cx45, analyzed by immunofluorescence, was not different in *Cx40*-deficient and wild-type heart (Figure 2e,f,i,j).

We performed ECG recordings — which give information about the heart beat and the rate of impulse conduction through the different regions of the heart — on wild-type, heterozygous and *Cx40*-deficient mice and measured the parameters defined in Figure 3a. Representative tracings are shown in Figure 3b. No significant differences in the frequency of heart beat were observed for *Cx40*$^{+/+}$ (487 ± 57 beats/min), *Cx40*$^{+/-}$ (506 ± 55 beats/min) and *Cx40*$^{-/-}$ (461 ± 65 beats/min) mice. Compared to *Cx40*$^{+/+}$

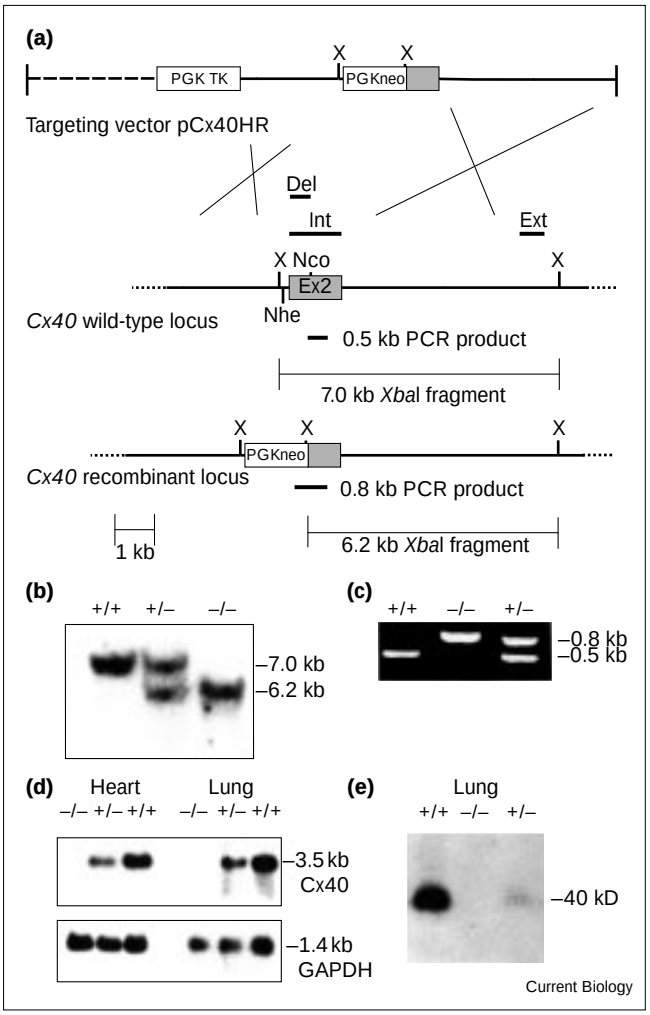

Figure 1

Targeted disruption of the mouse *Cx40* gene and expression analyses. (**a**) Targeting strategy. The targeting vector used (pCx40HR) included a herpes simplex virus (HSV) thymidine kinase cassette driven by the phosphoglycerate kinase promoter (PGK TK) and a neomycin-resistance cassette driven by the phosphoglycerate kinase promoter (PGKneo); the dashed line indicates DNA derived from pBR322 and the grey box indicates part of exon 2 of the *Cx40* gene. The complete reading frame of *Cx40* is encoded by exon 2 of the gene (grey box labelled Ex2). Restriction enzyme sites for *Xba*I (X), *Nco*I (Nco) and *Nhe*I (Nhe) are shown as are informative restriction enzyme fragments and PCR products. The Int probe (nucleotide position –33 to 1027 of mouse Cx40 cDNA [11]) and the Ext probe (0.6 kb *Hind*III genomic fragment) were used for Southern blot analysis. The Del probe (position –33 to 489 of mouse *Cx40* cDNA [11]) was used for northern blot analysis. (**b**) Southern blot analysis of *Xba*I-digested mouse DNA using the Int probe. (**c**) PCR analysis of mouse tail DNA. The wild-type allele resulted in the 0.5 kb band and the disrupted allele in the 0.8 kb band shown in (a). (**d**) Northern blot analysis comparing *Cx40* transcript abundancy in heart and lung of $Cx40^{-/-}$, $Cx40^{+/-}$ and $Cx40^{+/+}$ mice. After blotting, the same membrane was probed for *Cx40* using the Del probe shown in (a) and for human glyceroaldehyde 3-phosphate dehydrogenase (GAPDH), in order to show equivalent loading of the samples. (**e**) Immunoblot for Cx40 in samples (100 μg) enriched for gap junction plaques [4] from $Cx40^{+/+}$, $Cx40^{+/-}$ and $Cx40^{-/-}$ lungs.

and $Cx40^{+/-}$ mice, $Cx40^{-/-}$ mice showed prolonged intervals for all the ECG parameters tested (Table 1; P wave, +57%; PQ interval, +18%; QS interval, +46%; and QT_{max} interval, +50%). The P wave represents depolarization of the atrium, the PQ interval represents atrioventricular conduction, QS as well as QR intervals represent ventricular depolarization and the QT interval represents depolarization as well as repolarization of the ventricle. Thus, our data suggest that Cx40 is relevant to normal atrial,

Figure 2

Immunofluorescence analysis of cryostat sections of wild-type and *Cx40*-deficient hearts. Staining of wild-type (**a**,**c**,**e**) and $Cx40^{-/-}$ (**b**,**d**,**f**) coronary vessels. (a,b) The sections were incubated with anti-Cx40 antibody. (c,d) The same sections as in (a,b), respectively, were incubated with anti-PECAM (platelet endothelial cell adhesion molecule) antibody for specific labelling of endothelial cells. (e,f) Adjacent sections to those shown in (a,b) were incubated with anti-Cx37 antibody. Staining of wild-type (**g**) and $Cx40^{-/-}$ (**h–j**) atrium; the sections were incubated with either (g,h) anti-Cx40 antibody, (i) anti-Cx43 antibody or (j) anti-Cx45 antibody. The photographs in (b,h,j) were overexposed compared to those in the other panels in order to demonstrate nonspecific background fluorescence in (b,h) and the weak, specific signals (arrowheads) with anti-Cx45 antibody in (j). The magnification bar is 25 μm in (a–f) and 15.8 μm in (g–j).

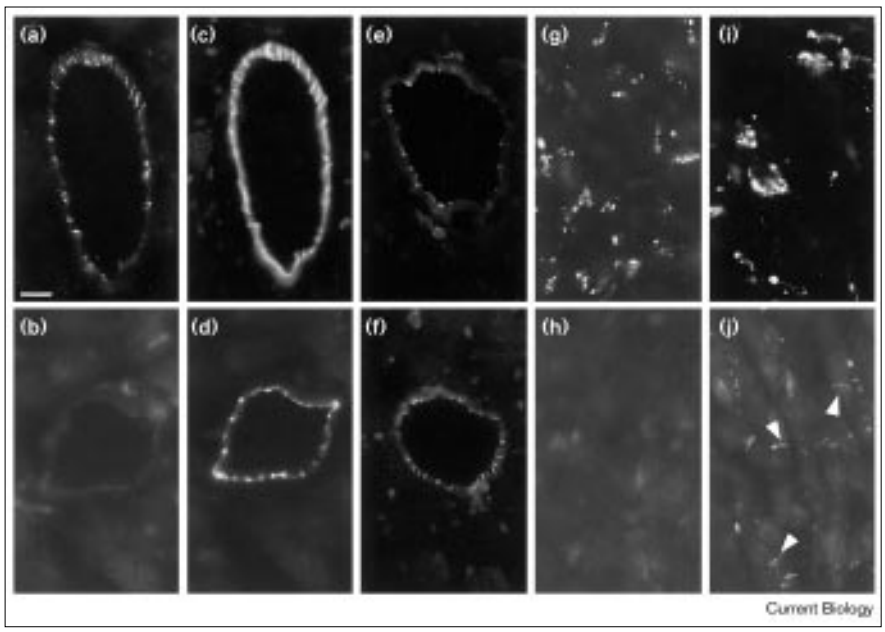

Figure 3

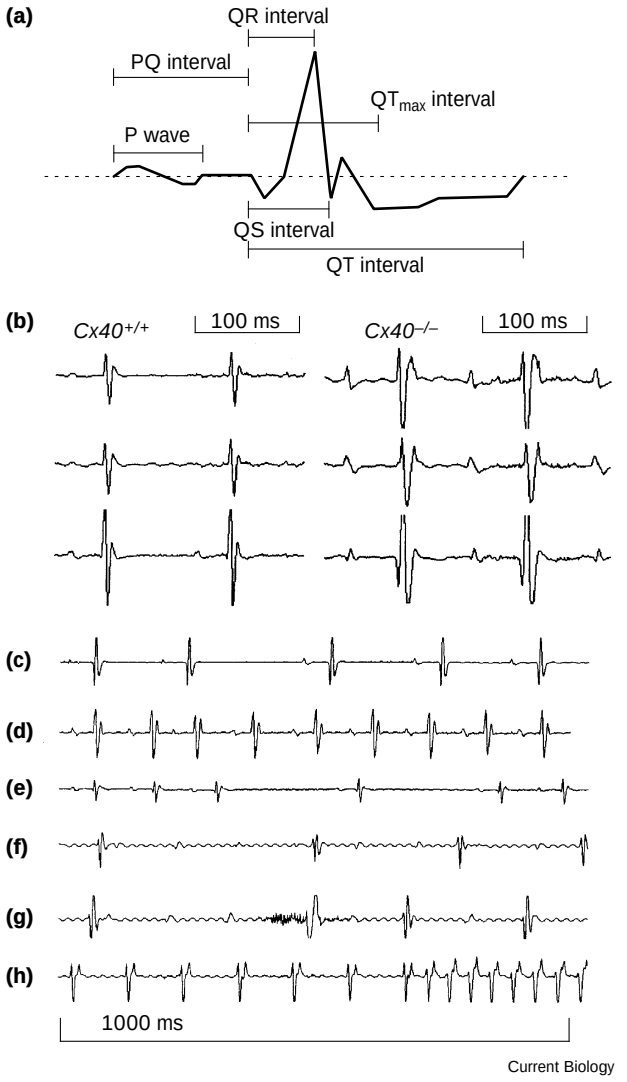

ECG recordings. (a) Schematic definition of the ECG parameters. (b) Representative ECG recordings from *Cx40*$^{+/+}$ and *Cx40*$^{-/-}$ mice. (c–h) Arrhythmias recorded in *Cx40*$^{-/-}$ mice: (c) sinus arrhythmia; (d) atrial ectopia (third P wave of the tracing); (e) sinus arrhythmia or sino-atrial block; (f) total AV block; (g) total AV block with ventricular ectopic beat; (h) intra-atrial re-entrant tachycardia.

atrioventricular and ventricular conduction velocities in the mouse. The hypothesis that myocytes connected via Cx40 channels may conduct action potentials more rapidly than cells connected by Cx43 channels [3,5,6] is confirmed by our data. In addition to their prolonged ECG parameters, 6 out of 31 *Cx40*-deficient mice examined displayed disturbances of pulse generation and/or sino-atrial and AV pulse propagation (Figure 3c–h), whereas no arrhythmias were found in the 26 *Cx40*$^{+/+}$ and 30 *Cx40*$^{+/-}$ mice examined. One *Cx40*$^{-/-}$ mouse showed high frequency intra-atrial re-entrant tachycardia. Thus, we

Table 1

Conduction parameters determined by ECG analysis of *Cx40*$^{+/+}$, *Cx40*$^{+/-}$ and *Cx40*$^{-/-}$ mice.

	Cx40$^{+/+}$	*Cx40*$^{+/-}$	*Cx40*$^{-/-}$
Number of mice	26	30	31
Cycle length (ms)	123.2 ± 16.2	118.5 ± 14.6	130.1 ± 21.3
P wave (ms)	16.0 ± 2.6*	16.2 ± 2.5†	25.1 ± 4.0
PQ interval (ms)	43.2 ± 4.7*	41.1 ± 5.6†	50.8 ± 7.8
QR intervals (ms)	6.8 ± 1.4*	7.3 ± 1.5†	9.9 ± 2.1
QS intervals (ms)	10.3 ± 1.8*	10.7 ± 1.6†	15.1 ± 3.4
QT$_{max}$ interval (ms)	16.0 ± 3.0*	17.0 ± 3.5†	24.3 ± 7.0
QT interval (ms)	31.8 ± 4.9*	31.9 ± 4.5†	45.5 ± 8.2

Statistical analysis showed that *$p < 0.05$ for *Cx40*$^{+/+}$ versus *Cx40*$^{-/-}$ and $^{\dagger}p < 0.05$ for *Cx40*$^{+/-}$ versus *Cx40*$^{-/-}$.

conclude that *Cx40* deficiency can be an important factor for arrhythmogenesis in the mouse.

In contrast to our results, in the accompanying report, Simon *et al.* [7] describe less extensive P-wave prolongation in their *Cx40*-deficient mice and no arrhythmias. Whereas differences of the P-wave length could be explained by differences in the definition of this parameter (see Figure 3a), the occurrence of arrhythmias might be influenced by differences in the mixed 129Sv/C57BL/6 genetic background of the mice investigated.

In humans, there are conflicting results about the expression of Cx40 in the AV node, the bundle branches and the Purkinje fibers of conductive myocardium, but it has been confirmed that Cx40 is expressed in the atrium and His bundle [8,9]. In patients with severe heart failure or myocardial hypertrophy, the distribution and abundance of Cx43 protein have been shown to be altered [10] and our results suggest that some patients with high-degree atrioventricular block and/or bundle branch block may lack functional Cx40 protein. Thus, further comparison of the functions and expression patterns of Cx40 in mouse and human heart may lead to an advance in the understanding of arrhythmogenesis in human patients.

Materials and methods

Targeted disruption of mouse Cx40 *gene*

A mouse 129/Sv genomic library (Stratagene) was screened with mouse *Cx40* cDNA [4]. The 5′ genomic 2.4 kb *Hind*III–*Nhe*I fragment and the 3′ genomic 5.1 kb *Nco*I fragment were cloned into a vector containing a PGKneo cassette and a PGK (HSV) TK cassette as shown in Figure 1. J1 embryonic stem cells [11], harbouring the correctly targeted allele, were injected into C57BL/6 mouse blastocysts. Chimeric males were bred with C57BL/6 females to yield germline transmission of the targeted allele. All analyses were done on littermates generated by interbreeding heterozygous *Cx40*-defective animals.

Northern blot hybridisation

Total RNA from adult tissues was collected using Trizol™ (Gibco BRL) according to the manufacturers' protocol and 20 µg each were electrophoresed and blotted on Hybond-N membrane (Amersham). Hybridization was performed using Quick Hyb® hybridisation solution (Stratagene) at 68°C. Filter washing and autoradiography were performed as described [12].

Southern blot analysis and PCR

Targeted embryonic stem cell clones and transgenic mice were analyzed by *Xba*I digestion of genomic DNA. After Southern blot hybridization, the external (Ext) probe (data not shown) and the internal (Int) probe recognized a 6.2 kb *Xba*I fragment of the targeted allele versus a 7.0 kb fragment of the wild-type allele (Figure 1a,b). A three-primer PCR analysis on mouse tail DNA was performed using the following primers: 5′-ATCAGGATGATCTGGACGAAGAGCATCAGG-3′ as 5′ primer for the recombinant locus, 5′-CAACACCTATGTCTGCACCATTCTGATCCG-3′ as 5′ primer for the wild-type locus and 5′-TACTCTGGCTTCTGGCTATAGTGCATGTGG-3′ as 3′ primer for both loci.

Protein isolation, immunoblot analysis and immunohistochemistry

Gap junction plaques were enriched by an alkali procedure [4] and subjected to standard immunoblot analysis using affinity purified rabbit anti-Cx40 [5], rabbit anti-Cx43 [5] and rabbit anti-Cx45 [13] antibodies, followed by incubation with ^{125}I-labelled protein A and autoradiography. Organs were frozen on dry ice. Frozen serial sections of 6 µm were fixed in absolute ethanol (–20°C) and immunolabelled with rabbit anti-Cx37 [13], rabbit anti-Cx40, rabbit anti-Cx43 or rabbit anti-Cx45 antibodies. Immunocomplexes were visualized using di-chlorotriacinyl-fluorescein (DTAF)-conjugated goat anti rabbit IgG (DIANOVA). For double immunofluorescence analysis, monoclonal rat anti-PECAM (Pharmingen) was added to anti-Cx40-Ig or anti-Cx37-Ig, respectively, and lissamine rhodamine (LRSC)-conjugated goat anti-rat IgG (DIANOVA) was added in the visualization step.

Electrocardiographic recordings

Mice were mildly anaesthesized by intraperitoneal injection of Avertin (Sigma; 1.25%, 0.02 ml per gram body weight). Electrodes were clipped cutaneously at each of the four limbs. Simultaneous six-lead ECG recordings were performed. The ECG amplifier sampled with a rate of 4 kHz. The data were stored at an optical disk (Bard Stamp™ Amplifier; Bard LabSystem Plus EP laboratory). P wave, PQ interval and QT interval were calculated by determining the earliest onset and the latest offset times from three simultaneously recorded surface leads. QR, QS and QT_{max} intervals were calculated from ECG tracings as displayed schematically in Figure 3a by measuring the onset time of the QRS complex and the maximum/minimum time of the R, and T waves. All values were expressed as the mean ± standard deviation. For statistical analysis, multivariate ANOVA with Scheffé's subgroup testing were performed. A p value < 0.05 was considered significant.

Acknowledgements

We thank F. Dombrowsky for microscopic comparison of *Cx40*$^{-/-}$ and *Cx40*$^{+/+}$ mouse hearts. This work has been supported by grants of the Deutsche Forschungsgemeinschaft (SFB 284, project C1), the Deutsche Krebshilfe, the Fond der Chemischen Industrie and the program BMH4-CT96-1427 of the European Community to K.W.

References

1. Kumar NM, Gilula NB: The gap junction communication channel. *Cell* 1996, 84:381-388.
2. Goodenough DA, Goliger JA, Paul DL: Connexins, connexons, and intercellular communication. *Annu Rev Biochem* 1996, 65:475-502.
3. Gros D, Jongsma HJ: Connexins in mammalian heart function. *Bioessays* 1996, 18:719-730.
4. Hertzberg EL: A detergent-independent procedure for the isolation of gap junctions from rat liver. *J Biol Chem* 1984, 259:9936-9943.
5. Traub O, Eckert R, Lichtenberg-Fraté H, Elfgang C, Bastide B, Scheidtmann KH, *et al.*: Immunochemical and electrophysiological characterization of murine connexin40 and -43 in mouse tissues and transfected human cells. *Eur J Cell Biol* 1994, 64:101-112.
6. Beblo DA, Wang HZ, Beyer EC, Westphale EM, Veenstra RD: Unique conductance, gating, and selective permeability properties of gap junction channels formed by connexin40. *Circ Res* 1995, 77:813-822.
7. Simon AM, Goodenough DA, Paul DL: Mice lacking connexin40 have cardiac conduction abnormalities characteristic of atrioventricular block and bundle branch block. *Curr Biol* 1998, 8:295-298.
8. Davis LM, Rodefeld ME, Green K, Beyer EC, Saffitz JE: Gap junction protein phenotypes of the human heart and conduction system. *J Cardiovasc Electrophysiol* 1995, 6:813-822.
9. van Kempen MJA, ten Velde I, Wessels A, Oosthoek PW, Gros D, Jongsma HJ, *et al.*: Differential connexin distribution accommodates cardiac function in different species. *Microsc Res Tech* 1995, 31:420-436.
10. Severs NJ: Pathophysiology of gap junctions in heart disease. *J Cardiovasc Electrophysiol* 1994, 5:462-475.
11. Li E, Bestor TH, Jaenisch R: Targeted mutation of the DNA methyltransferase gene results in embryonic lethality. *Cell* 1992, 69:915-926.
12. Hennemann H, Suchyna T, Lichtenberg-Fraté H, Jungbluth S, Dahl E, Schwarz J, *et al.*: Molecular cloning and functional expression of mouse connexin40, a second gap junction gene preferentially expressed in lung *J Cell Biol* 1992, 117:1299-1310.
13. Traub O, Butterweck A, Elfgang C, Hertlein B, Balzer K, Gergs U, *et al.*: Immunochemical characterisation of connexin31, -37, -40, -43, and -45 in cultured primary cells, transfected cell lines and murine tissues. *Prog Cell Res* 1995, 4:343-347.